Title: Morphological features of the testis among autoimmune mouse model and healthy strains

Zeinab Shouman[1,2,†], Hany El-Sayed Marei[1], Ahmed Abd-Elmaksoud[1], Mohammed Kassab[3], Takashi Namba[2], Md. Abdul Masum[2], Yasser Hosny Ali Elewa[2,4,†], Osamu Ichii[2,5], Yasuhiro Kon[2,*]

[1] Department of Cytology and Histology, Faculty of Veterinary Medicine, Mansoura University, Mansoura 35516, Egypt.

[2] Laboratory of Anatomy, Department of Biomedical Sciences, Faculty of Veterinary Medicine, Hokkaido University, Sapporo 060-0818, Japan.

[3] Department of Cytology and Histology, Faculty of Veterinary Medicine, Kafrelsheikh University, kafrelsheikh 33511, Egypt.

[4] Department of Histology and Cytology, Faculty of Veterinary Medicine, Zagazig University, Zagazig 44519, Egypt.

[5] Laboratory of Agrobiomedical Science, Faculty of Agriculture, Hokkaido University, Sapporo, Japan.

† Equally contributed author.

***Corresponding author**: Yasuhiro Kon, DVM, PhD, Laboratory of Anatomy, Department of Biomedical Sciences, Faculty of Veterinary Medicine, Hokkaido University, Kita 18, Nishi 9, Kita-ku, Sapporo 060-0818, Japan

Email: y-kon@vetmed.hokudai.ac.jp

Tel: +81-11-706-5187

Fax: +81-11-706-5189

Abstract

Autoimmune diseases play a critical role in the progression of infertility in both sexes and their severity has been reported to increase with age. However, few reports discussed their effect on the morphological features of the testis. Therefore, we compared the morphological alterations in the testes of autoimmune mice model (MRL/MpJ-Fas^{Lpr}) and its control strain (MRL/MpJ) with that of their background strain (C57BL/6N) at 3 and 6 months. Furthermore, we analyzed the changes in the meiotic spermatocytes, Sertoli cells, immune cells and junctional protein by immunohistochemical staining. The MRL/MpJ-Fas^{Lpr} mice showed a significant increase in the serum autoantibodies level, spleen/ body weight ratio and seminiferous luminal area when compared to other studied strains. On the other hand, a significant decrease in the testis/ body weight ratio, number of both Sertoli and meiotic spermatocyte was observed in MRL/MpJ-Fas^{Lpr} and MRL/MpJ mice than that in C57BL/6N mice especially at old age. However, neither immune cells infiltration nor significant difference in ZO-1 junctional protein expression could be observed among the studied strains. Our findings suggest that, the increase in autoimmune severity especially with age could lead to infertility through loss of spermatogenic and Sertoli cells, rather than disturbance of blood-testis barrier.

Keywords

Autoimmune disease, blood-testis barrier, MRL/MpJ-Fas^{Lpr} mice, seminiferous tubules, Sertoli cells, Testis.

Introduction

Recently, auto-immune diseases have gained researchers attention due to their association with occurrence of infertility in both sexes [1]. Systemic lupus erythematosus (SLE) is a systemic autoimmune disease in which multiple organs are affected and characterized by chronic activation of immune cells [2]. Despite the fact that female showed sever lesions than that of male in most of autoimmune diseases, few reports studied the effect of autoimmune disease on testicular morphology.

Autoimmune disease can cause autoimmune orchitis which can be classified to primary autoimmune orchitis that is completely related to antisperm antibody, and secondary autoimmune orchitis that is mainly caused by systemic autoimmune disease and 50 % related to antisperm antibody production besides causing apoptosis and loss of cells specially in SLE [3]. Previous studies showed sperms abnormality related to Sertoli cell dysfunction and decrease testis volume specially in SLE human patient [4,5]. However, studies related to morphological changes in the testicular structures associated with autoimmune diseases were scarce.

Currently, some autoimmune mouse models were utilized to elucidate the mechanisms beyond the progression of autoimmune associated lesions. Among these models, the BXSB/MpJ-Yaa (BXSB-Yaa) which have a mutant gene located on the Y chromosome accelerating the systemic autoimmune disease in male [6]. Recently, our team showed some histopathological abnormalities in the testis of the BXSB-Yaa mice (such as an increased number of both residual bodies and apoptotic germ cells in stage XII, and decreased number of Sertoli cell), and suggested their role in the pathogenesis of reproductive dysfunction in such autoimmune disease mice model [7]. However, no information on the morphological alterations associated with systemic autoimmune abnormality in the

66 testes of the autoimmune mice model used MRL/MpJ-Fas^{Lpr} (MRL/Lpr) which is a suitable model for
67 SLE characterized by the development of a systemic autoimmune disease similar to SLE from 3
68 months of age in both males and females involving several organs causing immune cells infiltration
69 and enlargement of different organs specially lymph nodes and spleen [8,9]. The MRL/MpJ mice are
70 the control strain of MRL/Lpr mice and show mild autoimmune disease in older ages [10]. As age is
71 a factor that affect autoimmune disease, the incidence of autoimmune disease is expected to increase
72 with age [11]. Furthermore, the C57BL/6N mice are considered healthy strain and the background
73 strain of the aforementioned mice [12].

74 Spermatogenesis is a very complicated process that includes 12 stages in mice [13]. It can
75 be affected by many factors, the alteration in such factors will cause imbalanced spermatogenesis [14].
76 The spermatogenic epithelium consists of Sertoli cells and spermatogenic germ cells (spermatogonia,
77 spermatocytes and spermatids), apoptosis of such cells is normal and continuously occurring to keep
78 a balanced cell number throughout lifetime [15]. Interestingly, the testes of MRL/MpJ mice showed 3
79 characteristic features including a metaphase-specific apoptosis during the first meiotic division [16],
80 heat-shock resistant spermatocytes [17] and a postnatal oocyte-like cells [18].

81 The knowledge of how systemic autoimmune disease histologically alter testis is limited [7],
82 therefore the present study was carried out to elucidate to what morphological extent the autoimmune
83 disease could alter the testicular structure through comparison between the autoimmune disease mice
84 model (MRL/Lpr), its control parent mice (MRL/MpJ) and its background mice (C57BL/6N) at 3 and
85 6 months of age providing insight into the pathogenesis of autoimmune disease associated infertility
86 in male.

Materials and methods

Animal

Mice were purchased from Japan SLC, Inc., (Shizuoka, Japan) and kept in the faculty of veterinary medicine's animal facility until they reached age of 3 months and 6 months, Four mice from each strain (C57BL/6N, MRL/MpJ, MRL/Lpr) at age of 3 months and 6 months were used, body weight was recorded, and then sacrificed under deep anesthesia of a mixture from butorphanol (0.5 mg/kg), midazolam (0.4 mg/kg) and medetomidine (3 mg/kg), according to the animal care and use of Hokkaido University, Faculty of Veterinary Medicine (approved by the Association for Assessment and Accreditation of Laboratory Animal Care International, approval No. 16-0124), and organs weight was recorded.

Autoimmune indices measurement

Serum of both MRL/Lpr and MRL/MpJ mice were collected and the double-strand DNA (dsDNA) levels were analyzed by Enzyme-Linked immunosorbent Assay (ELISA) using autoimmune disease ELISA kit (Fujifilm, cat no., AKRDD-061, according to manufacture procedures) (Um/mL). The spleen to body weight ratio was also compared among all studied strains.

Sample collection and tissue preparation

Right testes were removed and fixed by paraformaldehyde 4% (for immunohistochemistry and immunofluorescent staining) while left testes were removed and fixed with Bouin's solution (for tissue architecture examination and staging of seminiferous tubules). Testes were kept in fixative for more than 16 hours. Fixed testes were processed in ascending concentration of alcohol followed by xylene and immersed in paraffin wax then blocks were produced. The blocks were cut into 3μm thick paraffin sections and stained with hematoxylin-eosin (HE) to identify tissue architecture and periodic

111 acid Schiff combined with hematoxylin (PAS-H) to determine the seminiferous epithelial stage.

112

113 *Immunohistochemistry (IH) and Immunofluorescent (IF) staining*

114 Three µm thick sections were prepared on positively charged slides. Immunofluorescence
115 (IF) was performed using standard method. IF staining to detect Sertoli cells, and BTB junctional
116 protein using the following antibodies: GATA-binding protein 4 (GATA4) (Cat. No. sc-25310, Santa
117 Cruz, California, USA), Zonula occludens-1 (ZO1) (Cat. No. 339100, Invitrogen, California, USA)
118 respectively. Following deparaffinization the sections were subjected to antigen retrieval heating with
119 10 mM citrate buffer (pH 6.0) at 105˚C for 20 min using autoclave. Then they were washed with
120 distilled water and incubated with 5% normal donkey serum then the sections were washed with
121 phosphate buffer saline (PBS) with specific fluorescent for 3 times/5 min each and incubated overnight
122 with specific primary antibodies at 4˚C. The sections were washed in PBS and incubated with specific
123 fluorescent labelled secondary antibody for 30 mins (Table 1) followed by incubation with Hoechst
124 33342 solution (Do Jindo, Kumamoto, Japan) at dilution 1:2,000 for 2 mins. They were washed,
125 mounted and examined under a fluorescent microscope (BZ-X700, All-in-one Fluorescence Keyence,
126 Osaka, Japan).

127 Immunohistochemical (IH) staining to detect meiotic cells, macrophage, T cells, and B cells
128 using the following primary antibodies: Synaptonemal complex 3 (SCP3) (ab15093, Abcam,
129 Cambridge, UK), Iba1 (019-19741, Wako, Osaka, Japan), CD3 (413591F, Nichirei, Tokyo, Japan),
130 B220 (CL8990A, Cedarlane, Ontario, Canada). Following deparaffinization and rehydration, the
131 sections were subjected to antigen retrieval using the adequate condition for each antibody (Table1).
132 Then the sections were soaked in 0.3% H_2O_2 methanol for 20 mins to block the endogenous peroxidase
133 activity. They were washed in distilled water and incubated with the 10 % goat serum as blocking

serum at room temperature for one hour within humid chamber, followed by overnight incubation with the specific primary antibody. The sections were washed in PBS (3 times/ 5 mins) and incubated with the secondary antibodies for 1 hour at room temperature, washed again in PBS and incubated with streptavidin solution used for 30 minutes, and shortly incubated with 3,3′ diaminobenzidine tetrahydrate H_2O_2 (DAB) solution followed by rinsing in hematoxylin for 30 seconds and mounting. Images were taken using microscope (BZ-X700, All-in-one Fluorescence Keyence Microscope, Osaka, Japan**).**

Histometric analysis

For histometric analysis, testes from four mice were analyzed (2 sections from each mice) in all strains at both early (3 months) and late (6 months) age. The HE, PAS-H, and SCP3 immunostained sections were scanned by the nanozoomer scan machine (Hamamatsu photonics Co., ltd; Hamamatsu, Japan) and analyzed by nanozoomer digital pathology (NDP) view 2 software. The HE scanned sections were used to determine the average seminiferous tubule (ST) area, ST lumen area, ST epithelial area (ST lumen area subtracted from ST epithelial area) (Fig 2j). To determine the frequency of stages within ST, the ST within PAS stained testicular sections were examined and the stages were reported according to shape of acrosome and the existence of round spermatid as previously reported [19]. Furthermore, the numbers of SCP3 positive meiotic cells / ST area were calculated in nanozoomer scanned SCP3 immuno-stained sections by fixing the number of ST area from the 2 sections in all studied strains, counting cells in the ST area, and recording their average. Additionally, digital image from IF stained sections were analyzed by image J software (version 1.32J, http://rsb.information.nih.gov/iJ) to detect the GATA4 positive Sertoli cells /ST area, and the positive ZO-1 cell count. The later were measured by counting the positive cells per ST area [20].

Statistical analysis

Values are expressed as mean ± standard error. Data were analyzed by Kruskal-Wallis test to compare between the studied group followed by Scheffe's method for multiple comparison when significant difference among the group were observed ($P < 0.05$). Furthermore, correlation between two parameters were analyzed using Pearson's correlation test ($P < 0.05$; significant value and $P < 0.01$; highly significant value).

Results

Alteration in body weight, spleen weight and testis weight in examined strains

The 3 strains showed a variance in the average body weight that's why the relative weight of organs (organ weight to body weight) (Table 2) was considered. Spleen/body weight ratio showed a significant increase in MRL/Lpr mice at both 3 and 6 months furthermore, a tendency of increase in such ratio was observed in MRL/MpJ mice at 6 months. This was confirmed by measuring anti-dsDNA antibody level in MRL/Lpr and MRL/MpJ sera where a significant increase was observed in MRL/Lpr mice at 3 months when compared to its control strain (Fig 1a). Also, both strains showed an increased titer at 6 months than that of 3 months. This result was in accordance with the spleen weight to body weight ratio (Fig 1b).

Testis/body weight ratio showed a significant decrease in both MRL/Lpr and MRL/MpJ mice at 6 months of age and remained nearly the same in C57BL/6N mice compared to age of 3 months (Fig 1c). Pearson's correlation test showed a negative correlation between the testis/body weight ratio and the autoimmune disease indices (serum titer of dsDNA & spleen / body weight ratio) (Table 3).

Histological comparison of seminiferous tubules of the examined strains in both ages

Histologically, C57BL/6N mice (at both 3 and 6 months) and MRL/MpJ (at 3 months) mice showed normal regular seminiferous tubular architecture (Fig 2a,b,c) including normal ST lumina area, and epithelial area and ST area (Fig 2g-i). The average ST lumina area was 2034.2 μm in C57BL/6N mice at both 3 months, 6 months and 3797.6 μm in MRL/MpJ mice at 3 months. The average ST area was 29664.6 μm in C57BL/6N mice at both 3 months, 6 months and 37818.6 μm in MRL/MpJ mice at 3 months. The average ST epithelial area was 27630.4 μm in C57BL/6N mice at both 3 months, 6 months and 34021.1 μm in MRL/MpJ mice at 3 months. On the other hand, the testes of MRL/MpJ mice at 6 months and of MRL/Lpr mice at both 3 and 6 months of age showed altered morphological

features in their ST (Fig 2d-f). Such featured include the appearance of small vacuoles and/or spermatogenic cell loss in ST lumen. The STs of MRL/Lpr mice at 6 months of age, showed more dilation and wider luminal area with more spermatogenic cell loss and vacuolation (Fig 2f) than other studied groups. The average ST luminal area was 5069.3, 8840.9 and 8023.1 µm in MRL/Lpr mice at 3 months, 6 months and MRL/MpJ mice at 6 months, respectively. The average ST area was 37795.4, 44670.2 and 44662.5 µm in MRL/Lpr mice at 3 months, 6 months and MRL/MpJ mice at 6 months, respectively. The average ST epithelial area was 32726.2, 35829.3 and 36639.5 µm in MRL/Lpr mice at 3 months, 6 months and MRL/MpJ mice at 6 months, respectively. Furthermore, the STs of MRL/Lpr mice at 6 months of age showed significant higher values than that of C57BL/6N mice at both 3 months, 6 months and both MRL/MpJ and MRL/Lpr mice at 3 months.

Stage frequency in all studied strains

Staging of PAS stained STs was done to identify the frequency of every stage (Fig 3). Among all studied strains at both ages (Fig 3). The STs in all studied strains at 3 months as well as in C57BL/6N mice at 6 months showed high frequency for stages VII. However, a higher frequency for stage XII was observed in MRL/Lpr mice at 6 months and both stage III and XII in MRL/MpJ mice at 6 months.

Immunostaining of Junctional protein, Sertoli, and meiotic cells

To determine what kind of cell loss is associated with autoimmunity, counting of cells was carried out after performing both IF and IHC staining of different cell markers (SCP3 for meiotic cells, GATA4 for Sertoli cells) (Fig 4,5). The morphometrical measurement showed a significant decrease in SCP3 positive cells in all studied strains (Fig 4g). In addition, the Sertoli cells count in both MRL/Lpr and MRL/MpJ mice testis at 6 months showed a significant decrease than that of C57BL/6N

mice Furthermore, the C57BL/6N mice at 6 months showed a significant increase in the Sertoli cell count than that of 3 months (Fig 5h).

Immune cells infiltration and ZO-1 junction protein

To examine effect of autoimmunity on immune cell infiltration in testis and BTB, immunohistochemical staining was performed to detect both immune cells (CD3 for T cells, B220 for B cells, Iba1 for macrophages) and ZO-1 junctional protein as a major junctional protein for BTB. The ZO1 junctional protein appeared as whitish precipitates at the basal compartment of STs in sites of tight junction of BTB (Fig 5 a-f), it was counted in area of ST as well as in relation to Sertoli cells. Interestingly, a non-significant decrease in ZO-1^{+}cells/ST area was observed in testes of both MRL/MpJ and MRL/Lpr mice at 6 months than other studied groups (Fig 5g). Furthermore, in all studied strains our results revealed the presence of few CD3^{+} T lymphocytes, B220^{+} B lymphocytes and Iba1 macrophages in the interstitial tissue but there was no infiltration in the STs (Fig 6).

Furthermore, Pearson's correlation analysis revealed positive correlation between testis/body weight ratio and both Sertoli cell count and SCP3 positive meiotic cell count (Table 4). However, a negative correlation was observed between testis/body weight ratio and other morphometric measurement including ST area, ST lumen area, ST epithelial area, and ZO-1 positive cells /GATA4 positive cells.

Discussion and conclusion

In human, SLE is one of the autoimmune diseases that have great impact on the occurrence of infertility in both sexes. An abnormal semen was reported in human patient with SLE and owed that to Sertoli cells dysfunction due to decreased inhibin secretion from Sertoli cells [5]. Previous studies demonstrated a decrease in the testicular volume in SLE patients related to semen abnormalities and suggesting ST sever lesions [21]. Other reports suggested that the effect of autoimmunity on fertility could be due to disruption of immune privilege related to T cells reaction toward certain antigens [22]. However, the mechanism beyond the effect of autoimmunity on testicular integrity is not yet elucidated. Therefore, we examined the morphology of testes from MRL/Lpr mice that showed autoimmune disease at both early and late age as an attempt to investigate such mechanism. We also investigated the testes from MRL/MpJ mice that is known to develop an autoimmune disease at a later onset than MRL/Lpr mice [9] and compared with the testes of their healthy background strain (C57BL/6N mice) at both early (3 months) and late (6 months) age. The present investigation revealed higher autoimmune indices in MRL/Lpr mice at both ages with a significant increase in such indices in MRL/MpJ mice at 6 months, however, no difference in C57BL/6N mice at both ages. Therefore our results indicate that MRL/Lpr mice developed an autoimmune disease in both early and late age, but a mild autoimmune disease could be observed in MRL/MpJ mice in late age, however, no development of autoimmunity in C57BL/6N mice at both ages.

In parallel with the findings of Otsuka et, al. concerning the decrease in MRL/MpJ testis weight due to apoptosis [23], our investigation revealed high frequency of stage XI and XII within the ST of both MRL/Lpr and MRL/MpJ specially at 6 months that indicate apoptosis. Our report of a high frequency for stage VII in the ST of C57BL/6N mice in both ages could indicate normal fertility. Additionally, the present study elucidated that a significant decrease in testes weight associated with aging in both MRL/Lpr and MRL/MpJ mice as compared to C57BL/6N mice. Our result clarified that

such decrease in testes weight could be due to hollowness of the dilated ST lumen with germ cell loss and epithelial vacuolation. Similar results were also reported in passive experimental autoimmune orchitis [22].

Interestingly, SCP3 is considered a marker for meiotic cells (primary spermatocyte) [24], our study revealed a significant decrease in SCP3 positive cells in all studied strains in association with aging. Previous study showed that the decrease in meiotic cells was contributed to their apoptosis [25].

Our study revealed a significant decrease in GATA4 positive Sertoli cells in both MRL/Lpr and MRL/MpJ especially at 6 months but an increased value was detected in C57BL/6N mice. Such observation could be due to the effect of autoimmune disease in MRL/Lpr and MRL/MpJ but a normal age-related change in C57BL/6N mice. This was in parallel with previous report [26]. Furthermore, it has been revealed that the deletion of GATA4 leads to testicular atrophy and associated with development of infertility [27]. Interestingly, previous reports have been clarified the role of Sertoli cells in controlling the number of spermatogenic cells as well as the number of produced sperms [28, 29, 30]. Based on the aforementioned findings, we could suggest that the decrease in meiotic germ cells number in the current investigation is mainly due to the decrease in Sertoli cells number. Moreover, the loss of such germ cell could be attributed to apoptosis which is a main feature related to autoimmune orchitis [31].

The Fas system (Fas and FasL) has been reported to be involved in the induction of germ cell apoptosis [32, 33]. Furthermore, it has been recorded that there was an increase in metaphase specific apoptotic cells in MRL/MpJ mice testis in comparison to C57BL/6N mice testis in stage XII [16]. Similarly, our results revealed increased frequency of stage XII in both MRL/Lpr and MRL/MpJ mice testis at 6 months suggesting an increased apoptosis in such strains.

Additionally, in order to examine the involvement of immune cells infiltration and the

disturbance in BTB with the morphological alteration of testes of studied strains, we examined the infiltration of various immune cells (B, T lymphocytes and macrophages) as well as the disturbance in BTB junctional protein ZO-1 expression which is considered as a major component of BTB tight junctional protein. Our result revealed absence of immune cells infiltration in STs in all studied strains which is in accordance with previous report [34]. However, a non-significant decrease in ZO-1 protein expression in STs of MRL/MpJ and MRL/Lpr mice especially with old age. Previous report revealed a disturbance of BTB as a result of destruction of ZO-1 protein [35].

In conclusion, the testis of autoimmune disease mice model MRL/Lpr and its parent strain MRL/MpJ mice showed a decreased weight and an altered histological feature as compared to their background strain C57BL/6N especially at 6 months of age at which the autoimmune disease progressed including dilated ST with hollowness (wide lumen) and vacuolated epithelium suggested that the effect of autoimmune disease could be through loss of germ cells through apoptosis rather than their effect on immune cells infiltration or BTB disturbance.

Acknowledgments and funding

This research was supported by Egypt-Japan Education Partnership (EJEP) joint supervision scholarship.

Declaration of Interest

The present manuscript was approved by all authors to be submitted to Experimental animal journal and was not submitted to other journal, so we declare that there are no conflicts of interest.

Abbreviations

SLE systemic lupus erythematosus

Fas L Fas Ligand

HE hematoxylin-eosin HE

PAS-H periodic acid Schiff combined with hematoxylin

dsDNA double stranded DNA

ST seminiferous tubules

IH immunohistochemistry

IF immunofluorescent

GATA4 GATA -Binding Protein 4

SCP3 Synaptonemal complex protein 3

ZO-1 Zonula occludens-1

BTB blood-testis barrier

References

1. Carp HJA. Selmi C, Shoenfeld Y. The autoimmune bases of infertility and pregnancy loss. Journal of Autoimmunity 2012: 38(2–3), J266-J274.
2. Ray S, Sonthalia N, Kundu S, et al. Autoimmune Disorders: An Overview of Molecular and Cellular Basis in Today's Perspective. J Clin Cell Immuno. 2012; 2215-2230.
3. Silva CA, Coccuzza M, Carvahlo JF, et al. Diagnosis and classification of autoimmune orchitis. Autoimmunity Rev. 2014;13: 431–434
4. Soares PMF, Borba EF, Bonfa E, et al. Gonad Evaluation in Male Systemic Lupus Erythematosus. Arthritis and rheumat. 2007; 56(7): 2352–2361.
5. Suehiro RM, Borba EF, Bonfa1 E, et al. Testicular Sertoli cell function in male systemic lupus erythematosus. Rheumatol. 2008; 47:1692–1697.
6. Izui S, Merino R, Fossati L, Iwamoto M. The role of the Yaa gene in lupus syndrome. Int Rev Immunol. 1994;11(3):211-230.
7. Otani Y, Ichii O, Masum MA, et al. BXSB/MpJ-Yaa mouse model of systemic autoimmune disease shows increased apoptotic germ cells in stage XII of the seminiferous epithelial cycle. Cell and Tissue Research. 2020;10.1007/s0041-020-03190-0.
8. Perry D, Sang A, Yin Y, et al. Review Article Murine Models of Systemic Lupus Erythematosus.

J Biomed Biotechnol. 2010; 2011: 271694.

9. Hewicker M, Kromschroder E, Trautwein G. Detection of circulating immune complexes in MRL mice with different forms of glomerulonephritis. Z Versuchstierkd. 1990;33(4):149-56.
10. Hang L, Aguado MT, Dixon FJ, et al. Induction of severe autoimmune disease in normal mice by simultaneous action of multiple immunostimulators. J Exper Med. 1985; 161: 423-428.
11. Goronzy JJ, Weyand CM. Immune aging and autoimmunity. Cell. Mol. Life Sci. 2012: 69:1615–1623.
12. Kalley VE, Roths JB. Interaction of mutant lpr gene with background strain influences renal disease. Clin immnopatol. 1985;37(2):220-229.
13. Leblond CP, Clermont Y. Definition of the stages of the cycle of the seminiferous epithelium in the rat. Ann N Y Acad Sci. 1952; 55: 548-573.
14. de Kretser DM, Loveland KL, Meinhardt A, et al. Spermatogenesis. Hum Reproduct. 1998; 13(
15. Moreno RD, Reyes JG, Farías JG, et al. Spermatogenesis at the extreme: oxidative stress as a converging mechanism of testicular damage due to pathological and environmental exposure. Testis: Anat Physiol Pathol. 2012; chapter 1.
16. Kon Y, Endoh D. Morphological study of metaphase-specific apoptosis in MRL mouse testis. Anat Histol Embryol. 2000;29(5):313-319.
17. Namiki Y, Kon Y, Kazusa K, et al. Quantitative trait loci analysis of heat stress resistance of spermatocytes in the MRL/MpJ mouse. Mamm Genome. 2005;16(2):96-102.
18. Otsuka S, Konno A, Hashimoto Y, et al. Oocytes in newborn MRL mouse testes. Biol Reprod. 2008;79(1):9-16.
19. Ahmed EA, de Rooij DG. Staging of Mouse Seminiferous Tubule Cross-Sections. Meiosis, Volume 2: Cytological Meth. 2009; 558.

20. Tripathi UK, Chhillar S, Kumaresan A, et al. Morphometric evaluation of seminiferous tubule and proportionate numerical analysis of Sertoli and spermatogenic cells indicate differences between crossbred and purebred bulls. Vet. World. 2015; EISSN: 2231-0916.
21. da Silva CAA, Bonfá E, EF Borba, et al. Reproductive health in male systemic lupus erythematosus. Bras J Rheumatol. 2009; 49(3):207-227.
22. lhng KSK, Teuscher C. Mechanisms of autoimmune disease in the testis and ovary. Human Reproduc Update. 1995; 1(1) 35-50.
23. Otsuka S, Namiki Y, Ichii, O et al. Analysis of factors decreasing testis weight in MRL mice, Mamm Genome. 2010; 21(3-4): 153-161.
24. Heyting C. Synaptonemal Complexes: Structure and function. Curr. Opin. Cell Biol. 1996; 8: 389-396.
25. Yuan L, Liu J-G, Zhao J, et al. The Murine SCP3 Gene Is Required for Synaptonemal Complex Assembly, Chromosome Synapsis, and Male Fertility. Molecular Cell. 2000; 5: 73–83.
26. Takano H, Kazuhiro ABE. Age-related histologic changes in the adult mouse testis. Arch histol jap. 1987; 50(5): 533-544.
27. Kyrönlahti A, Euler R, Bielinska M, et al. GATA4 regulates Sertoli cell function and fertility in adult male mice. Molecul Cellul Endocrinol. 2011; 333: 85-95.
28. Johnson L, Thompson JrDL, Varner DD. Role of Sertoli cell number and function on regulation of spermatogenesis. Anim Reprod Sci. 2008; 105:23–51.
29. Johnson L, Zane RS, Petty CS, et al. Quantification of the human Sertoli cell population: Its distribution, relation to germ cell numbers, and age-related decline. Biol Reprod. 1984. 31:758–795.
30. Sharpe RM, McKinnell C, Kivlin C, et al. Proliferation and functional maturation of Sertoli cells, and their relevance to disorders of testis function in adulthood. Reprod. 2003; 125:769–

784.

31. Jacobo P, Guazzone VA, Theas MS, et al. Testicular autoimmunity. Autoimmun Rev. 2011; 10: 201–204.
32. Riccioli A, Salvati L, D'Alessio A, et al. The Fas system in the seminiferous epithelium and its possible extra-testicular role. Andrologia, 2003; 35: 64–70.
33. lee J, Richburg JH, Younkin SC, et al. The Fas system is a key regulator of germ cell apoptosis in the testis. Endoc Soc. 1997; 138: 5.
34. Fanning AS, Jameson BJ, Jesaitis LA, et al. The tight junction protein ZO-1 establishes a link between the transmembrane protein occludin and the actin cytoskeleton. J Biol Chem. 1998; 273: 29745–29753.
35. Wittchen ES, Haskins J, Stevenson BR. Protein interactions at the tight junction. Actin has multiple binding partners, and ZO-1 forms independent complexes with ZO-2 and ZO-3. J Biol Chem. 1999; 274: 35179–35185.

Figure legends

Figure 1: Charts showing spleen weight to body weight ratio with a significant increase in MRL/Lpr mice compared to MRL/MpJ and C57BL/6N mice (a). A significant increase in dsDNa antibody level in MRL/Lpr mice compared to MRL/MpJ mice (b) and testis weight to body weight ratio with significant decrease in both MRL/MpJ and MRL/Lpr mice compared to C57BL/6N mice (c). Data was analyzed by Kruskal-Wallis test followed by Scheffe's method ($P < 0.05$), n=4 in each experimental group. The letters a, b, c, d, e and f significant difference between groups (a=C57BL/6N 3m, b=MRL/MpJ 3m, c=MRL/Lpr 3m, d=C57BL/6N 6m, e=MRL/MpJ 6m, f=MRL/Lpr 6m). Values are given as mean ±SE.

Figure 2: Photomicrograph of H&E staining of Bouins fixed C57BL/6N ST at 3 months (a) and 6 months (b) showing a regular ST architecture, MRL/MpJ ST at 3 months (c) and 6 months (d) showing

a regular tubules that altered to wide lumen dilated ST with vacuolation (arrow heads) at 6 months of age, and MRL/Lpr ST at 3 months (e) some showed regular tubules while other showed loss of cells (arrows) which gathered in lumen and beginning of epithelial vacuolation (arrow heads) and 6 months (f) showed wide lumen dilated ST with vacuolated epithelium (arrow heads), the chart (g,h,i) shows the average ratio of luminal, tubular and epithelial area in all studied strains and j shows the area measured for lumen and ST. Data was analyzed by Kruskal-Wallis test followed by Scheffe's method ($P < 0.05$), n=4 in each experimental group. The letters a, b, c, d, e and f significant difference between groups (a=C57BL/6N 3m, b=MRL/MpJ 3m, c=MRL/Lpr 3m, d=C57BL/6N 6m, e=MRL/MpJ 6m, f=MRL/Lpr 6m). Values are given as mean ±SE. scale bars=100µm.

Figure 3: Photomicrograph of PAS staining of Bouins fixed C57BL/6N ST at 3 months (a) and 6 months (b), MRL/MpJ ST at 3 months (c) and 6 months (d), and MRL/Lpr ST at 3 months (e) and 6 months (f), while charts (g) and (h) show frequency of stage occurrence in all strains in which all strains showed highest occurrence of stage 7 at 3 months of age, while at age of 6 months C57BL/6N showed frequent occurrence of stage 7, MRL/MpJ mice showed frequent occurrence of stage 3 and stage 12 and MRL/Lpr mice showed frequent occurrence of stage). Data was analyzed by Kruskal-Wallis test followed by Scheffe's method ($P < 0.05$), n=4 in each experimental group. The letters a, b, c, d, e and f significant difference between groups (a=C57BL/6N 3m, b=MRL/MpJ 3m, c=MRL/Lpr 3m, d=C57BL/6N 6m, e=MRL/MpJ 6m, f=MRL/Lpr 6m). Values are given as mean ±SE. scale bars=100µm.

Figure 4: NDP Photomicrograph of immunohistochemistry staining against SCP3 of C57BL/6N ST at 3 months (a) and 6 months (b), MRL/MpJ ST at 3 months (c) and 6 months (d), and MRL/Lpr ST at 3 months (e) and 6 months (f), the positive reaction was observed as brown reaction in the nucleus of spermatocytes (arrow heads), while chart (g) shows counting of +ve cells/area in all studied strains. Data was analyzed by Kruskal-Wallis test followed by Scheffe's method ($P < 0.05$), n=4 in each

experimental group. The letters a, b, c, d, e and f significant difference between groups (a=C57BL/6N 3m, b=MRL/MpJ 3m, c=MRL/Lpr 3m, d=C57BL/6N 6m, e=MRL/MpJ 6m, f=MRL/Lpr 6m). Values are given as mean ±SE. scale bars=25µm.

Figure 5: Photomicrograph of immunofluorescence staining of ZO-1 (white), GATA4 (red) and Hoechst (blue) in C57BL/6N ST at 3 months (a) and 6 months (b), MRL/MpJ ST at 3 months (c) and 6 months (d), and MRL/Lpr ST at 3 months (e) and 6 months (f), while chart (g) shows counting of ZO-1 positive cells in ST area in all studied strains. Data was analyzed by Kruskal-Wallis test followed by Scheffe's method ($P < 0.05$), n=4 in each experimental group. The letters a, b, c, d, e and f significant difference between groups (a=C57BL/6N 3m, b=MRL/MpJ 3m, c=MRL/Lpr 3m, d=C57BL/6N 6m, e=MRL/MpJ 6m, f=MRL/Lpr 6m). Values are given as mean ±SE. scale bars=100µm for low magnification and 30µm for magnified inset.

Figure 6: NDP photomicrograph of immunohistochemical staining of MRL/Lpr mice STs for CD3, B220 and Iba1 at 6 months of age showing no infiltration of such cells in the STs.

Tables

Table 1: Antibodies used in immunostaining, expressing cells, dilution, antigen retreival method, secondary antibody, blocking serum and method.

Primary antibody	Target cell	Dilution	Antigen retrieval method	Secondary antibody
GATA4 (goat)	Sertoli cells and interstitial cells besides nonspecific reaction in acrosome	1:100	10 mM CB (pH 6.0) 105℃ for 20 minutes	anti-goat-IgG (produced in donkey) Alexa Fluor 546, Santa Cruz, USA
SCP3 (rabbit)	Meiotic cell	1:750	10 mM CB (pH 6.0)105℃ for 20 minutes	anti-Rabbit IgG (produced in goat) biotin labelled (H1903,Histofine)
ZO-1 (rabbit)	BTB junctional protein (Sertoli cell)	1:500	10 mM CB (pH 6.0) 105℃ for 20 minutes	anti-rabbit-IgG (produced in donkey) Alexa Fluor 647, Santa Cruz, USA

Iba1 (rabbit)	Macrophage	1:200	0.3 % Pepsin 37℃ for 5 minutes	anti-Rabbit IgG (produced in goat) biotin labelled (H1903,Histofine)
CD3 (rabbit)	T lymphocytes	1:100	10 mM CB (pH 6.0) 105℃ for 20 minutes	anti-Rabbit IgG (produced in goat) biotin labelled (H1903,Histofine)
B220 (Mouse)	B lymphocytes	1:1600	0.3 % Pepsin 37℃ for 5 minutes	anti-mouse IgG (produced in goat) biotin labelled (H1605, Histofine)

Table 2: Shows the average body weight, average spleen weight/body weight, and average testis weight/body weight in all studied strains.

	Average Body weight (gm)		Average Spleen weight /body weight		Average Testis weight/body weight	
	3 M	6 M	3 M	6 M	3 M	6 M
C57BL/6N	24.9425	29.6875	0.003141	0.003129	0.00705	0.00701
MRL/MpJ	45.8345	46.244	0.001977	0.002225	0.004409	0.004127
MRL/Lpr	45.01225	52.64625	0.005943	0.015105	0.003828	0.003569

Table 3: Pearson correlation between autoimmune indices (spleen weight/Body weight and dsDNA antibody level) and testis weight to body weight ratio.

		Testis weight/Body weight
Spleen weight/Body weight	ρ	-0.528
	P	0.078
dsDNA antibody level	ρ	-.644*
	P	0.024

*Significant, P <0.05.

449 **Table 4:** Pearson correlation between testis weight to body weight ratio (Testis/Body weight) and

450 other morphometric measurement.

		ST luminal area	ST area	ST epithelial area	$SCP3^{+}$ cells/area	StageXII	Zo-1/GATA4	GATA4/area (Sertoli cells)
Testis / Body weight	ρ	-.839**	-.837**	-.722**	0.033	-.608**	-.0463	0.561*
	p	0.001	0.001	0.001	0.895	0.007	0.053	0.016

451 *Significant, P <0.05 while ** highly significant, P <0.01.

a

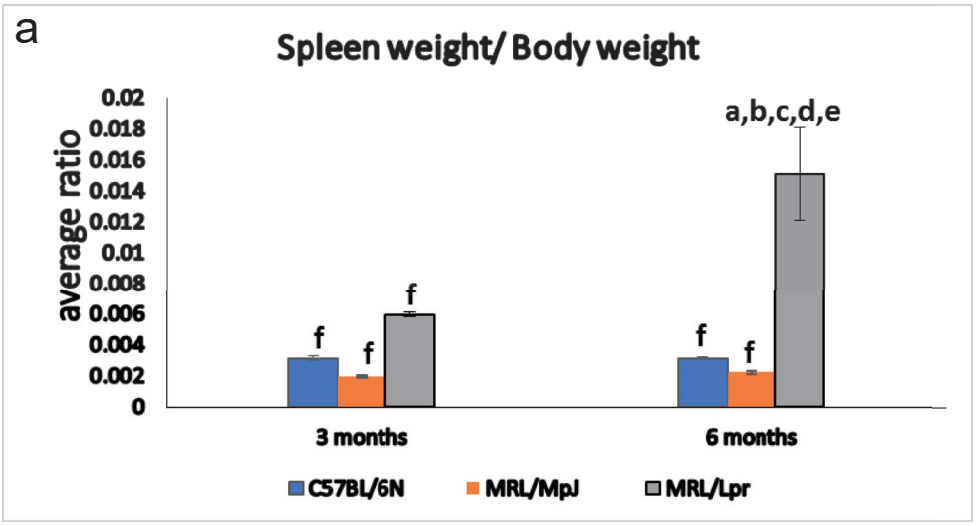
Spleen weight/ Body weight
average ratio
0.02
0.018
0.016
0.014
0.012
0.01
0.008
0.006
0.004
0.002
0
f
f
f
f
f
a,b,c,d,e
3 months
6 months
C57BL/6N
MRL/MpJ
MRL/Lpr

b

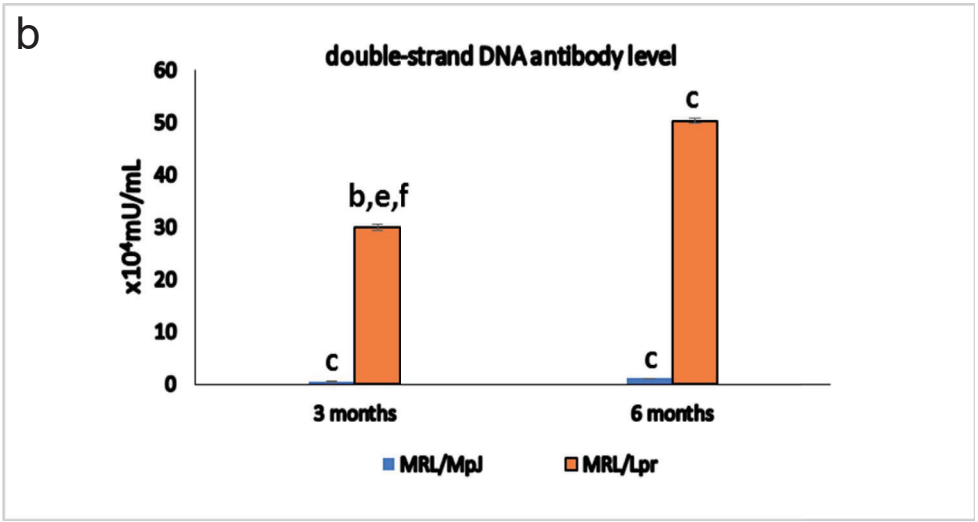
double-strand DNA antibody level
x10⁴mU/mL
60
50
40
30
20
10
0
c
b,e,f
c
c
3 months
6 months
MRL/MpJ
MRL/Lpr

c

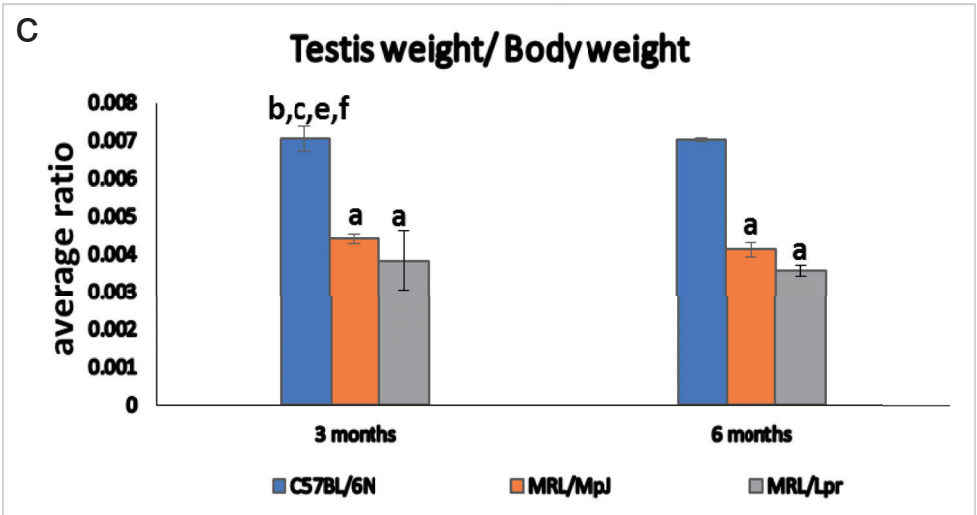
Testis weight/ Body weight
average ratio
0.008
0.007
0.006
0.005
0.004
0.003
0.002
0.001
0
b,c,e,f
a
a
a
a
3 months
6 months
C57BL/6N
MRL/MpJ
MRL/Lpr

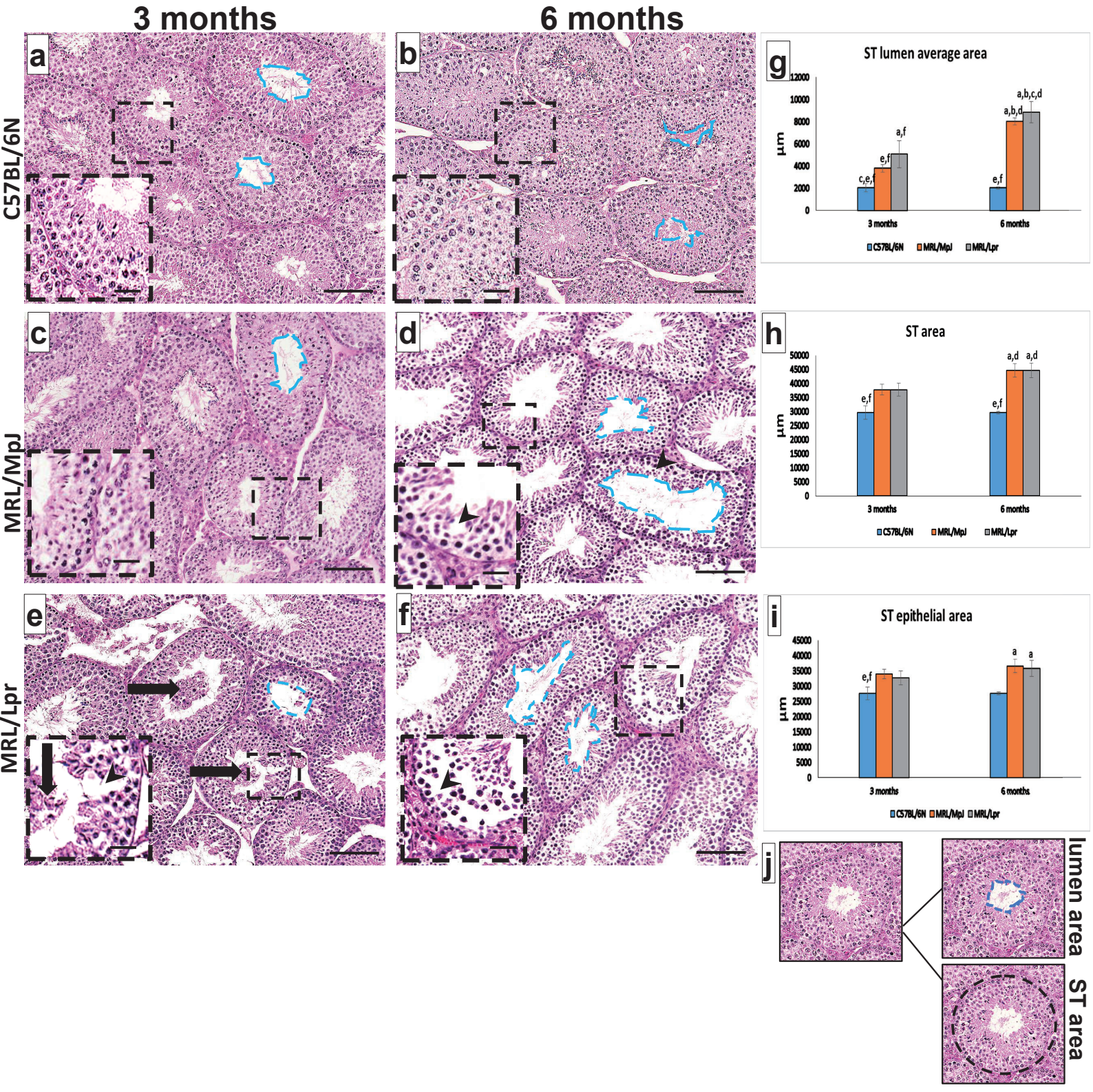
3 months
6 months
C57BL/6N
MRL/MpJ
MRL/Lpr
a
b
c
d
e
f
g
ST lumen average area
µm
12000
10000
8000
6000
4000
2000
0
c,e,f
e,f
a,f
e,f
a,b,d
a,b,c,d
3 months
6 months
C57BL/6N
MRL/MpJ
MRL/Lpr
h
ST area
50000
45000
40000
35000
30000
25000
20000
15000
10000
5000
0
e,f
e,f
a,d
a,d
i
ST epithelial area
45000
40000
35000
30000
25000
20000
15000
10000
5000
0
e,f
a
a
j
lumen area
ST area

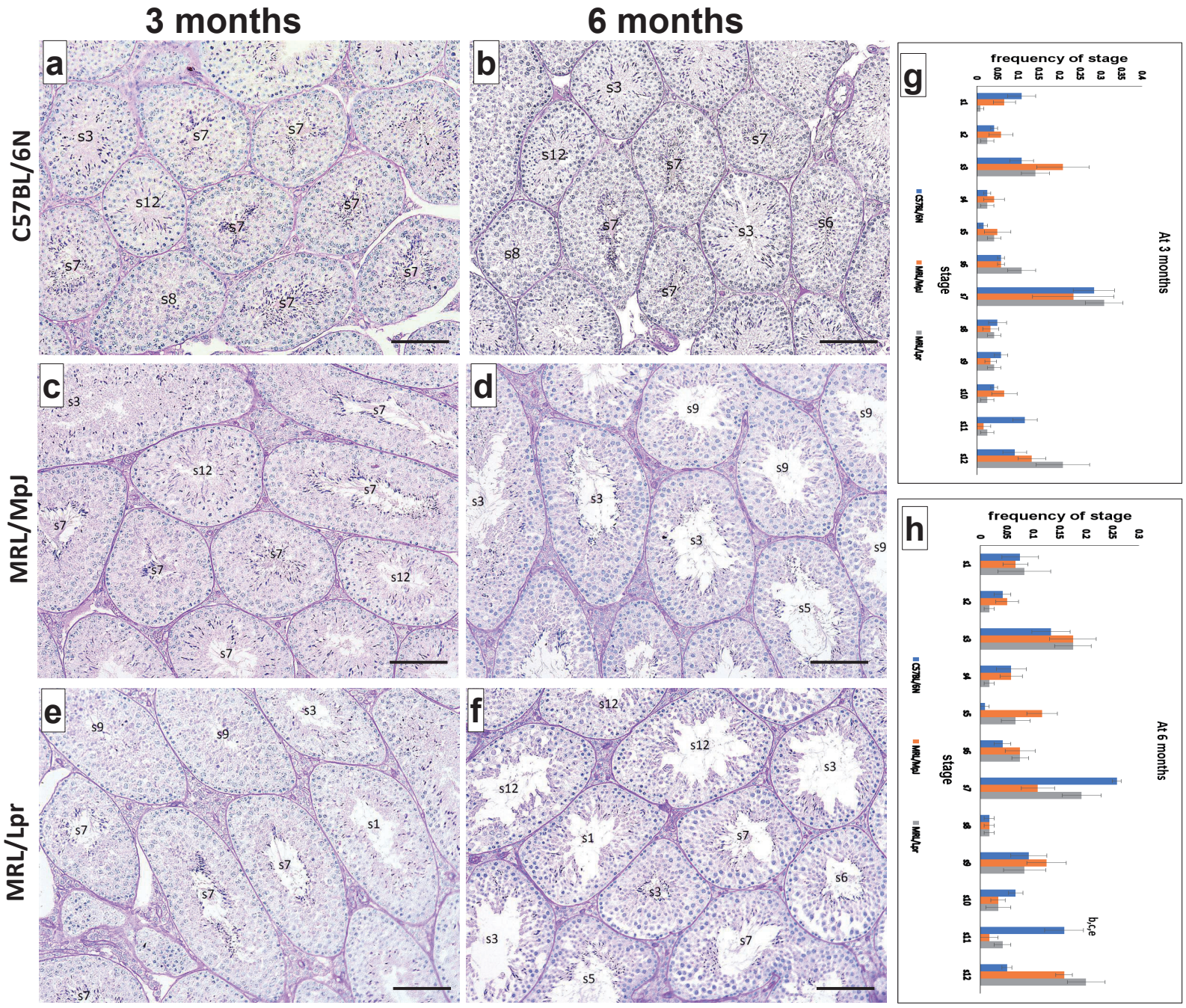
3 months
6 months
C57BL/6N
MRL/MpJ
MRL/Lpr
a
b
c
d
e
f
g
h
s3
s7
s12
s8
s9
s1
s6
s5
frequency of stage
stage
At 3 months
At 6 months
b,c,e

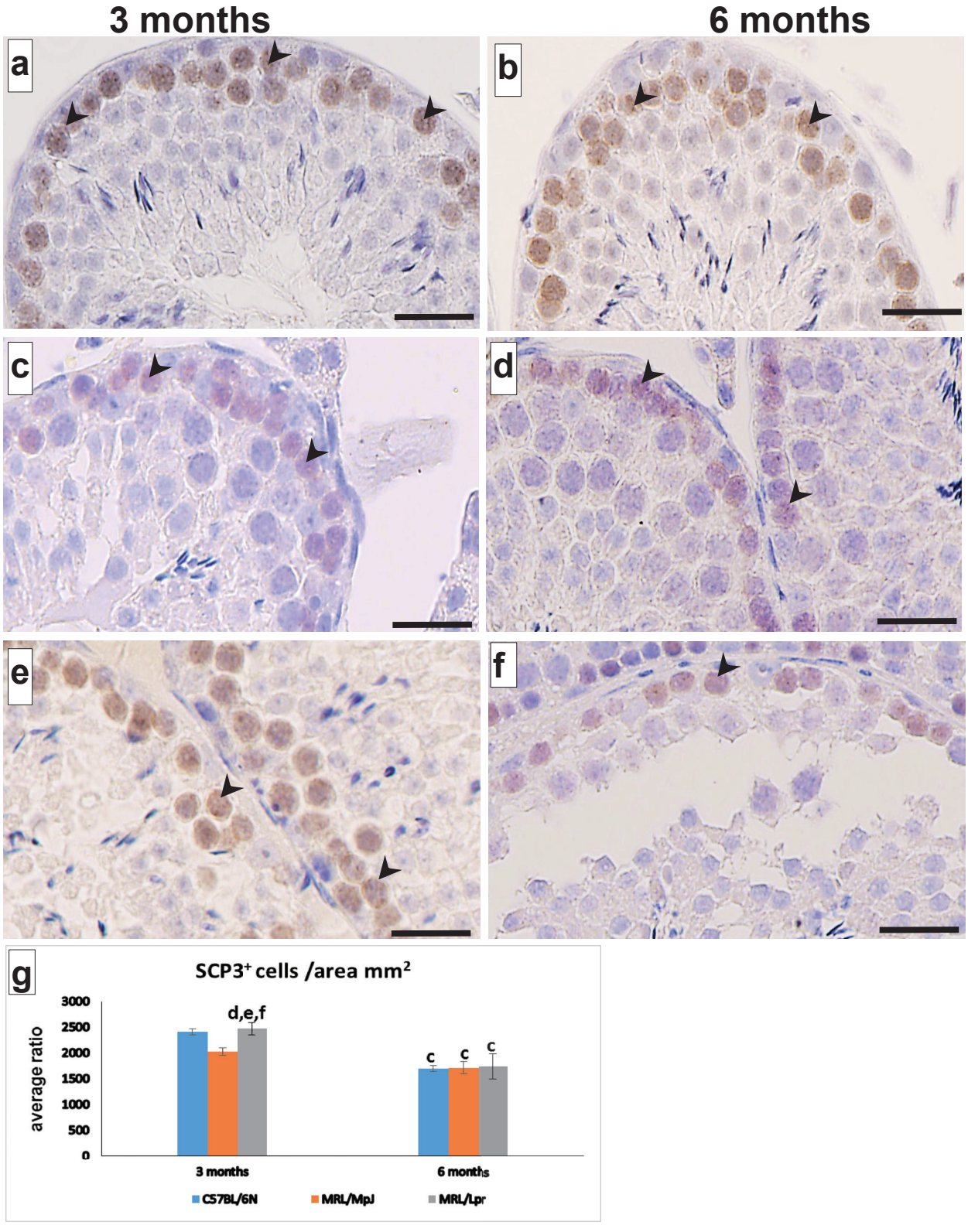
3 months
6 months
C57BL/6N
MRL/MpJ
MRL/Lpr
a
b
c
d
e
f
g
SCP3+ cells /area mm2
average ratio
3000
2500
2000
1500
1000
500
0
d,e,f
c
c
c
3 months
6 months
C57BL/6N
MRL/MpJ
MRL/Lpr

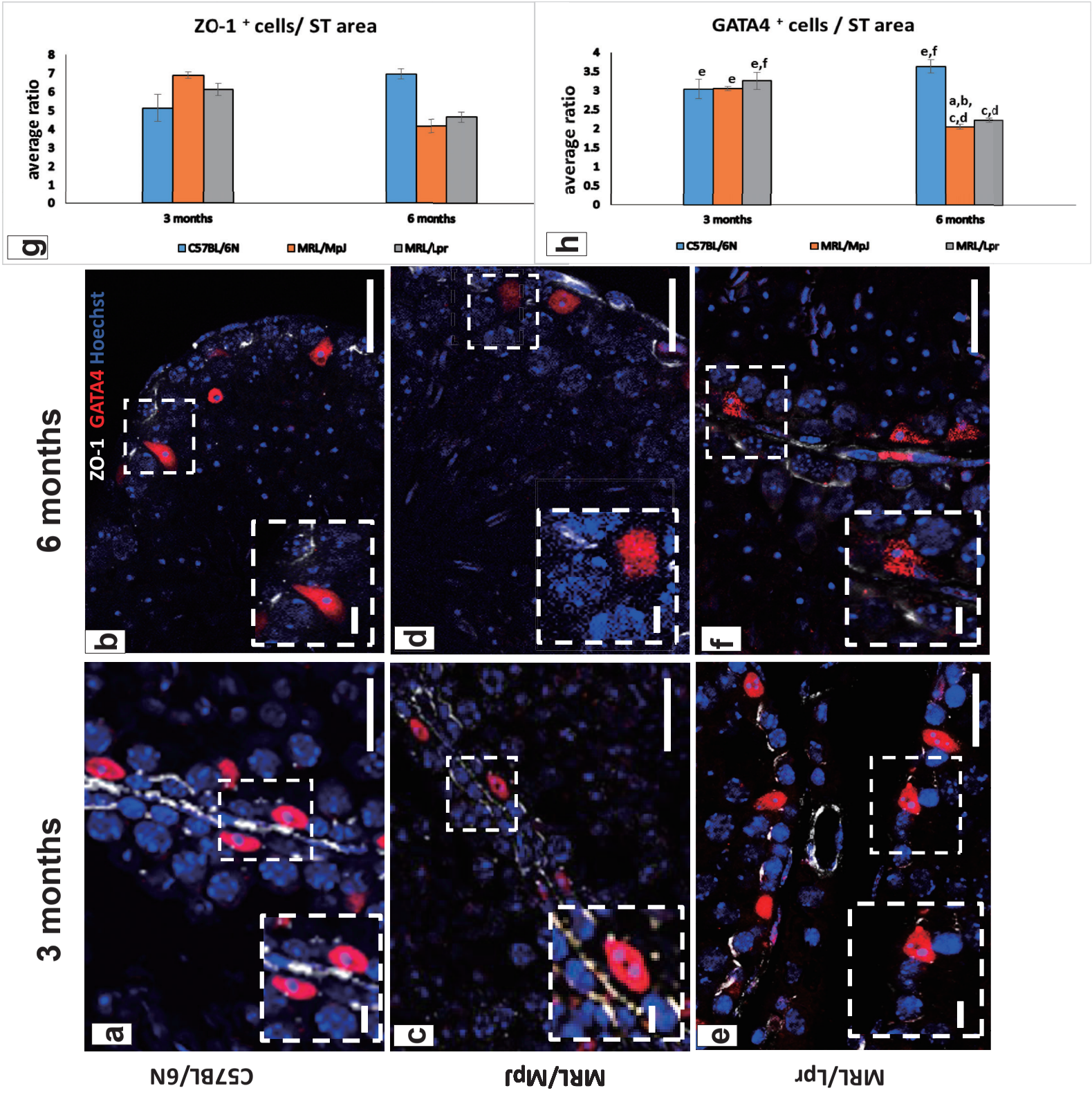
ZO-1 + cells/ ST area
average ratio
3 months
6 months
C57BL/6N
MRL/MpJ
MRL/Lpr
g
GATA4 + cells / ST area
e
e
e,f
e,f
a,b, c,d
c,d
h
ZO-1 GATA4 Hoechst
6 months
3 months
b
d
f
a
c
e
C57BL/6N
MRL/Mpj
MRL/Lpr

MRL/Lpr 6 months